

# Field Theoretical Approach to Electrochemical Deposition\*

H. A. Taroco, A. L. Mota<sup>†</sup>

Departamento de Ciências Naturais, Universidade Federal de  
*São João del Rei*  
Caixa Postal 110, CEP 36.301-160, São João del Rei, MG,  
*Brazil*

In this work we present an application of the  $\lambda\phi^4$  field theoretical model to the adsorption of atoms and molecules on metallic surfaces - the electrochemical deposition. The usual approach to this system consists in the computational simulation using Monte Carlo techniques of an effective lattice-gas Hamiltonian. We construct an effective model towards a comparison between the lattice-gas Hamiltonian and the discrete version of the  $\lambda\phi^4$  Hamiltonian, obtaining the relationships between the model parameters and electrochemical quantities. The  $\lambda\phi^4$  model is studied in the mean field approximation, and the results are fitted and compared to numerical simulated and experimental data.

## I. INTRODUCTION

There is a recent convergence on the subjects of studies and techniques of electrochemistry and surface science. In particular, the processes where ions and molecules are deposited over a metallic surface can be treated with both analytical or numerical statistical mechanics techniques. These processes are of fundamental interest since it presents detailed aspects of the electrode-electrolyte interface structure. Electrical current and potential for electrochemical deposition in metallic surfaces are obtained by cyclic voltammetry, showing current peaks in a determined potential range. The shape, position and number of these peaks depends on the surface where the deposition occurs, as well as on the electrolyte nature. The peaks are related to phase transitions of the adsorbed layers ([1], [2]), and this aspect makes this electrochemical subject be well adapted to statistical mechanics studies.

The dynamics of the adsorption of atoms and molecules on metallic surfaces in electrolytic solutions due to voltage differences - the electrochemical deposition - can be described, in an effective way, by the lattice-gas model. In this model, the adsorption of an element (adsorbed specie) changes the energy of the system due the bound energy of the element to the surface, and due lateral interactions between adsorbed species. The system is described by a Hamiltonian that reproduces interaction between nearest neighbors (but not only first nearest neighbors) and terms relative to an external field (adsorbed specie electrochemical's potential). The Hamiltonian is usually treated by using computational simulation, such as Monte Carlo simulations, in both equilibrium ([3]- [6]) and quasi-equilibrium situations ([7]- [9]), reproducing surface coverage and voltammetric current profiles in good agreement with experimental data. Also analytical treatment is employed in these systems ([10]- [16]). However, in contrast with the first ones, these treatments usually employ some empiric approximations.

The analytical treatment of this model is quite difficult, since it involves up to fifth neighbors interactions [9], characterizing the non-local nature of the model. Another aspect that increases the complexity of these treatments arises when we consider potential terms of order higher than quadratic. In fact, those higher order potential terms are usually avoided.

The continuous limit of the discrete lattice-gas Hamiltonian is a field theoretical model. In the treatment of such model, there's no great difficulties, although requiring perturbative expansions, in dealing with higher order potential terms. Nevertheless, non-local terms in field theoretical models are of difficult treatment, and as long as it can be done, one looks always for local field theoretical models.

In this work we present a field theoretical model constructed from the continuous version of the electrochemical deposition lattice-gas Hamiltonian. To avoid non-local terms, we will consider only first nearest neighbors interactions, but, in order to reproduce the phase transition presented by the electrochemical deposition, we will introduce a fourth order potential term, leading to the  $\lambda\phi^4$  model.

We must remark, nevertheless, as indicated in [17], that the numerical Monte Carlo treatment of such systems has some advantages in the detailed description of the surfaces, of the distribution and sizes of deposited ions and

---

\*Supported by CAPES-Brazil

<sup>†</sup>motaal@ufsj.edu.br

molecules, and so on. But an analytical, or specifically, a field theoretical description of the electrochemical deposition process can improve the understanding of the phenomena involved, since it provides simple analytical expressions for some of the observable quantities and gives a comprehensible description of how the symmetry breaking is related to the phase transition of the system. It also opens the possibilities for the study of the presence of topological solutions (solitons and vortices) in the distribution of the adsorbed specie over the electrode surface, which, in future, could represent the possibility of new technological features.

## II. CONTINUOUS VERSION OF THE LATTICE-GAS MODEL

Let us start from the grand-canonical lattice-gas Hamiltonian ([4], [5], [9]) for the electrochemical deposition of one specie in a square lattice, given by

$$H = -J \sum_{i,j=1}^N \{c_{i,j}c_{i,j+1} + c_{i,j}c_{i+1,j}\} + \mu \sum_{i,j=1}^N c_{i,j} + H_3, \quad (1)$$

where  $J$  is the lateral interaction between species occupying nearest neighbors sites,  $c_{i,j} = \{0, 1\}$  denotes the occupation of sites labeled by its row and column numbers  $i$  and  $j$ ,  $\mu$  is the electrochemical potential and  $H_3$  is higher order interaction terms. The electrochemical potential  $\mu$  is related to the electrode potential through:

$$\mu = \mu_0 + kT \ln \frac{C}{C_0} - e\gamma V, \quad (2)$$

where  $C_0$  is some reference value for the specie concentration in solution,  $\mu_0$  is the electrochemical potential at the reference concentration and zero electrode potential  $V$ ,  $C$  is the specie concentration in solution and  $\gamma$  is the electrovalence of the specie.

The thermodynamic conjugate to the electrochemical potential is the surface coverage  $\Theta$ , that represents the fraction of occupied sites

$$\Theta = N^{-1} \sum_{i=0}^N c_i \quad (3)$$

, where  $N$  is the total number of unity cells in the electrode surface. The charge transported through the substrate/electrode interface in adsorption/desorption process is given by

$$q = -e\gamma\Theta, \quad (4)$$

and the voltammetric current density (voltammetric current per adsorption site) can be obtained from its derivative

$$i = \frac{dq}{dt} = -e\gamma \frac{d\Theta}{dt} = -e\gamma \frac{d\theta}{d\mu} \frac{d\mu}{dV} \frac{dV}{dt}, \quad (5)$$

where we express eq. (5) as a function of the scan rate  $\frac{dV}{dt}$ .

Rewriting (1) by using a symmetric occupation number  $\phi_{i,j}$ , given by

$$\phi_{i,j} = 2c_{i,j} - 1; \quad \phi_{i,j} = \{-1, +1\} \quad (6)$$

we find

$$H = -\frac{J}{4} \sum_{i,j=1}^N (\phi_{i,j}\phi_{i,j+1} + \phi_{i,j}\phi_{i+1,j}) - \left(-J + \frac{\mu}{2}\right) \sum_{i,j=1}^N \phi_{i,j} + H_3 \quad (7)$$

where we had made use of periodic boundary conditions. Introducing the interaction strength by unitary cell  $\frac{J}{a^2}$ , where  $a$  is the lattice spacing and  $a^2$  is the unitary cell area, we find

$$H = -\frac{J}{4a^2} \sum_{i,j=1}^N a^2 \{\phi_{i,j}\phi_{i,j+1} + \phi_{i,j}\phi_{i+1,j}\} - \frac{-J + \mu/2}{a^2} \sum_{i,j=1}^N a^2 \phi_{i,j} + H_3 \quad (8)$$

or

$$H = -\frac{J}{4a^2} \sum_{i,j=1}^N a^2 \left\{ \left( -\frac{1}{2}\phi_{i,j}^2 + \phi_{i,j}\phi_{i,j+1} - \frac{1}{2}\phi_{i,j+1}^2 \right) + \left( -\frac{1}{2}\phi_{i,j}^2 + \phi_{i,j}\phi_{i+1,j} - \frac{1}{2}\phi_{i+1,j}^2 \right) \right\} \quad (9)$$

$$- \frac{Jz}{16a^2} \sum_{i,j=1}^N a^2 \left\{ \phi_{i,j}^2 + \frac{1}{2}\phi_{i,j+1}^2 + \frac{1}{2}\phi_{i+1,j}^2 \right\} - \frac{-J + \mu/2}{a^2} \sum_{i,j=1}^N a^2 \phi_{i,j} + H_3.$$

where  $z$  is the number of nearest neighbors to the site  $i, j$ .

Applying the periodic boundary conditions, eq. (9) reduces to

$$H = \frac{J}{8} \sum_{i,j=1}^N a^2 \left\{ \left( \frac{\phi_{i,j} - \phi_{i,j+1}}{a} \right)^2 + \left( \frac{\phi_{i,j} - \phi_{i+1,j}}{a} \right)^2 \right\} \quad (10)$$

$$- \frac{Jz}{8a^2} \sum_{i,j=1}^N a^2 \phi_{i,j}^2 - \frac{-J + \mu/2}{a^2} \sum_{i,j=1}^N a^2 \phi_{i,j} + H_3.$$

In order to obtain a field model that corresponds to (10), we must assume that the lattice spacing is negligible when compared to the lattice dimensions, and that the occupation number of neighbors sites changes slowly from one site to another. In fact, as stated by eq. (6),  $\phi_{i,j}$  can assume only one of two discrete values,  $\pm 1$ . To obtain a genuine field theory, we must replace the occupation number  $\phi_{i,j}$  in eq. (10) by its configurational mean  $\phi(x, y) = \langle \phi_{i,j} \rangle$ , where the brackets represents the mean over all configurations allowed to the system at certain fixed conditions (temperature, solute concentration, electrode potential). Since cyclic voltammetry is carried out with slow scan rates, in a quasi-statical procedure, it seems to be reasonable that all allowed states with some fixed energy could contribute to a specific current measurement.

Denoting  $H$  and  $\phi$  for the configurational mean hamiltonian and occupation number respectively from now on, we can take the limit  $a \rightarrow 0$ , and replace the lattice columns and rows labels  $i$  and  $j$  by the sites positions  $x$  and  $y$ , resulting in

$$H = \int dx dy \left\{ \frac{J}{8} \left( \vec{\nabla} \phi \right)^2 - \frac{Jz}{8a^2} \phi^2 - \frac{-J + \mu/2}{a^2} \phi \right\} + H_3 = \int dx dy h, \quad (11)$$

where  $\phi = \phi(x, y)$ . Identifying the Hamiltonian density  $h$ , we found

$$h = \frac{J}{8} \left( \vec{\nabla} \phi \right)^2 - \frac{Jz}{8a^2} \phi^2 - \frac{-J + \mu/2}{a^2} \phi + h_3, \quad (12)$$

where  $h_3$  is the Hamiltonian density of the higher order interaction terms, and

$$H_3 = \int dx dy h_3. \quad (13)$$

By applying the appropriate Legendre transformation, we obtain the Lagrangian density for the continuous model

$$l = -\frac{1}{2} \frac{J}{4} \left( \vec{\nabla} \phi \right)^2 - \frac{1}{2} \left( -\frac{Jz}{4a^2} \right) \phi^2 + \frac{-J + \mu/2}{a^2} \phi - h_3. \quad (14)$$

Here, we are also neglecting higher order correlations, i.e., we are assuming  $\langle \phi^2 \rangle = \langle \phi \rangle^2$ .

Rewriting the Lagrangian density in terms of

$$\varphi = \frac{\sqrt{J}}{2} \phi \quad (15)$$

we obtain

$$l = -\frac{1}{2} \left( \vec{\nabla} \varphi \right)^2 - \frac{1}{2} \left( -\frac{z}{a^2} \right) \varphi^2 + \frac{-2J + \mu}{a^2 \sqrt{J}} \varphi - h_3. \quad (16)$$

Finally, defining the quantities  $m$  and  $c$  by

$$m^2 = -\frac{z}{a^2}, \quad (17)$$

and

$$c = \frac{2J - \mu}{a^2 \sqrt{J}}, \quad (18)$$

we obtain, for the Lagrangian density of the continuous extension of the lattice gas Hamiltonian applied to the electrochemical deposition,

$$l = -\frac{1}{2} \left( \vec{\nabla} \varphi \right)^2 - \frac{1}{2} m^2 \varphi^2 + c\varphi - h_3, \quad (19)$$

formally identical to a scalar field model with a symmetry breaking term. The quantities appearing in (19) are related to the lattice gas model effective quantities through eq. (6),(15),(17) and (18).

The surface coverage, given by eq. (3), can be given in this continuous version of the lattice-gas model by

$$\Theta = N^{-1} \sum_{i=1}^N c_i = N^{-1} J^{-1/2} \sum \varphi_i + \frac{1}{2} = N^{-1} a^{-2} J^{-1/2} \int dx dy \varphi(x, y) + \frac{1}{2}, \quad (20)$$

where we have made use of (6) and (15).

The model described by (19) corresponds to the non-linear sigma model, since it is restricted, by means of eq. (6), to  $-1 \leq \phi \leq 1$ , which implies in

$$-\frac{\sqrt{J}}{2} \leq \varphi \leq \frac{\sqrt{J}}{2}. \quad (21)$$

In this work we are interested in the description of the phase transition in electrochemical deposition, which occurs in the region far from saturation ( $\varphi = \pm \sqrt{J}/2$ ). Thus, we will treat the  $\varphi$  as a non-restricted field, keeping in mind that the results will be valid only in the region where  $|\varphi| < \sqrt{J}/2$ .

### III. THE $\lambda\varphi^4$ MODEL IN THE MEAN FIELD APPROXIMATION

From eq. (19) we can see that, with vanishing breaking term and higher order interactions, the Lagrangian for the continuous version of the lattice gas model presents a symmetry related to the exchange of the occupation number  $\varphi \rightarrow -\varphi$ . Since the transition between the state where the adsorption of the specie is favored and the state where desorption is favored is dictated by the electrode potential, present in the explicit symmetry breaking term (18), we assume that the higher order interaction terms will be also symmetric to the exchange of the occupation number, and thus only even order terms must be present in  $h_3$ . The lowest even order interaction term is the  $\varphi^4$ , and we will assume

$$h_3 = \frac{\lambda}{4!a^2} \varphi^4, \quad (22)$$

where  $\lambda$  is the coupling constant and  $a^2$  was inserted here for dimensionality reasons. By this relationship, we are assuming that the potential energy of the system is non-quadratic in  $\varphi$ . From (19) and (22) we obtain

$$l = -\frac{1}{2} \left( \vec{\nabla} \varphi \right)^2 - \frac{1}{2} m^2 \varphi^2 + c\varphi - \frac{\lambda}{4!a^2} \varphi^4, \quad (23)$$

the  $\lambda\varphi^4$  model with an explicit symmetry breaking term. Due the fact that the mass term in (23) is positive, since  $m^2$  is negative (17), the model presents spontaneous symmetry break in the limit  $c = 0$ . In this limit, the minimum of the potential energy in (23) occurs in

$$\varphi_{\min} = \sqrt{-\frac{3!m^2a^2}{\lambda}} \equiv \eta \quad (24)$$

or

$$\varphi_{\min} = -\sqrt{-\frac{3!m^2a^2}{\lambda}}.$$

Perturbative solutions must be constructed around one of these minima. Introducing the shifted field  $\varphi_s = \varphi - \eta$  in the Lagrangian (23), we find

$$l = -\frac{1}{2} \left( \vec{\nabla} \varphi_s \right)^2 - \left( \frac{1}{2} m^2 + \frac{6\eta^2 \lambda}{4!a^2} \right) \varphi_s^2 + \left( c - m^2 \eta - \frac{\eta^3 \lambda}{3!a^2} \right) \varphi_s - \frac{\eta \lambda}{3!} \varphi_s^3 - \frac{\lambda}{4!a^2} \varphi_s^4. \quad (25)$$

Lagrangian (25) is no longer symmetric in the sense that it is not invariant under the exchange  $\varphi_s = -\varphi_s$ , so the model shows an spontaneous symmetry breakdown. The potential energy minimum occurs now at the point  $\varphi_s = 0$ . Applying the Euler-Lagrange equations

$$\vec{\nabla} \left( \frac{\partial l}{\partial(\vec{\nabla} \varphi_s)} \right) - \frac{\partial l}{\partial \varphi_s} = 0 \quad (26)$$

in (25), we obtain, for the dynamic equation of the system,

$$-\nabla^2 \varphi_s = -\frac{\lambda}{6a^2} \varphi_s^3 - \frac{\lambda \eta}{2a^2} \varphi_s^2 - 2 \left( \frac{\lambda \eta^2}{4a^2} + \frac{m^2}{2} \right) \varphi_s + \left( -\frac{\eta^3 \lambda}{6a^2} - m^2 \eta + c \right). \quad (27)$$

We can proceed the solution of eq. (27) perturbatively around  $\varphi_s = 0$ . Thus, expanding  $\varphi_s$  as a power series of a perturbative parameter  $\varepsilon$ , i.e.,  $\varphi_s = \varphi_0 + \varepsilon \varphi_1 + \varepsilon^2 \varphi_2 + \dots$ , with  $\varphi_0 = 0$ , and keeping only the lowest order terms ( $\varepsilon^0$ ) implies in

$$-\frac{\eta^3 \lambda}{6a^2} - m^2 \eta + c = 0 \quad (28)$$

, a cubic equation that can be solved analytically for  $\eta$ . As showed in figure 1, equation (28) presents one (figures 1a I and III) or three real solutions (figure 1a II), for the potential energy as a function of  $\varphi_s$ , corresponding to the local minimum or maximum. Stability is granted for the global minimum, for  $c = 0$  we have two symmetric global minima, but for  $c \neq 0$  the system has this symmetry explicitly broken, as one can see from figures 1b - 1d. Thus, in  $c = 0$  the system presents a transition between one global minimum to another.

Solutions to equation (28) is given analytically by

$$\eta_1 = \frac{\Delta^{1/3}}{\lambda} - \frac{2m^2 a^2}{\Delta^{1/3}}, \quad (29)$$

$$\eta_2 = \left( -\frac{\Delta^{1/3}}{2\lambda} + \frac{m^2 a^2}{\Delta^{1/3}} \right) + \sqrt{3}i \left( \frac{\Delta^{1/3}}{2\lambda} + \frac{m^2 a^2}{\Delta^{1/3}} \right) \quad (30)$$

and

$$\eta_3 = \left( -\frac{\Delta^{1/3}}{2\lambda} + \frac{m^2 a^2}{\Delta^{1/3}} \right) - \sqrt{3}i \left( \frac{\Delta^{1/3}}{2\lambda} + \frac{m^2 a^2}{\Delta^{1/3}} \right), \quad (31)$$

with

$$\Delta = 3ca^2 \lambda^2 + \lambda^2 \sqrt{\frac{8m^6 a^6 + 9c^2 a^4 \lambda}{\lambda}}. \quad (32)$$

We must observe that solutions (29), (30) and (31) are independent of the unitary cell area, since it appears only in the combinations  $m^2 a^2$  and  $ca^2$ , and, due (17) and (18)

$$m^2 a^2 = -\frac{z}{a^2} a^2 = -z \quad (33)$$

and

$$c a^2 = \frac{2J - \mu}{a^2 \sqrt{J}} a^2 = \frac{2J - \mu}{\sqrt{J}}. \quad (34)$$

Thus, the number of free parameters of the model is reduced for only four: the electrochemical potential  $\mu$ , the effective lateral interaction  $J$ , the strength of the non-quadratic local interaction  $\lambda$  and the effective electrovalence of the adsorbed specie  $\gamma$ . The latter is also limited into a range of values near the electrovalence of the adsorbed specie.

First order ( $\varepsilon^1$ ) solutions to (27) implies in

$$\nabla^2 \varphi_1 = \left( \frac{\lambda \eta^2}{2} + m^2 \right) \varphi_1. \quad (35)$$

Solutions of eq. (35) can improve the results presented in this work, with oscillatory solutions around the mean solution  $\varphi_0$ .

#### IV. SOFT BREAK LIMIT

In the limit of vanishing  $c$ , solutions to eq. (28) reduces to

$$\eta_{c=0} = 0; \quad \eta_{c=0} = \pm \sqrt{\frac{-6m^2 a^2}{\lambda}}. \quad (36)$$

For very small  $c$ , we must suppose  $\eta = \eta_{c=0} + \delta$ , where  $\delta$  is a small perturbation around the  $c = 0$  solution. Replacing these perturbative solution in eq.(28) and retaining only first order terms in  $\delta$ , one can find

$$\eta_{\pm} = \pm \sqrt{\frac{-6m^2 a^2}{\lambda}} - \frac{c}{2m^2}. \quad (37)$$

This approximate solution for  $\eta$  allows us to obtain some simple estimative expressions for the voltammetric current and surface coverage that guide us in the initial parameters choice for the non-linear fitting of the model to the experimental data. The physical measurable parameters are the electrode potential  $V$ , the scan rate  $dV/dt$ , the voltammetric current  $i$  and the surface coverage  $\Theta$ .

The energy of the system in the state represented by solution (37) can be read from eq. (25). The solution that represents the global minimum energy switches from  $\eta_+$  to  $\eta_-$  when  $c$  runs from negative to positive values. The electrode potential at the transition point, obtained from (18) and (2) for  $c = 0$  is given by

$$V_c = \frac{-2J + \mu_{0C}}{e\gamma}, \quad (38)$$

where we call  $\mu_{0C} = \mu_0 + kT \ln(C/C_0)$ , the electrochemical potential at solute concentration  $C$  and temperature  $T$ . The current at the transition point can be obtained from (5), where the intermediate derivatives can be obtained from (18) and (2), and, from (28), we have

$$-\frac{\lambda}{2a^2} \eta^2 d\eta - m^2 d\eta + dc = 0 \quad (39)$$

i.e.

$$\frac{d\eta}{dc} = \frac{2}{\lambda m^2 / a^2 + 2m^2}. \quad (40)$$

Replacing these results in (5), we obtain

$$i = \frac{e^2 \gamma^2}{J} \frac{2}{\lambda \eta^2 + 2m^2 a^2} \frac{dV}{dt}, \quad (41)$$

a result that is not restricted to the soft break limit.

At the transition point, where  $\eta$  is given by the non zero solutions of (36), replacing (17), we obtain

$$i_C = \frac{e^2 \gamma^2}{8J} \frac{dV}{dt}. \quad (42)$$

Near  $c = 0$ , with  $\eta$  given by (36),  $i^{-1}$  is quadratic in  $V$ , as one can see from (41), (37),(18) and (2). The critical electrode potential can be evaluated by means of eq. (2) and (18) with  $c = 0$ .

The fact that  $i^{-1}$  is quadratic in  $V$  near the critical point, together with eq. (38) and (42) can be used to set the initial guess parameters for a non-linear fitting of eq. (41) to experimental data.

## V. NUMERICAL RESULTS

Voltammetric current and surface coverage for the process of electrodeposition of one single adsorbed specie on a square-lattice metallic surface at constant temperature and solute concentration can be reproduced in lowest order of the mean field approximation by equations (41) and (20). The free parameters of the model are  $J$ ,  $\mu_{0C}$ ,  $\lambda$  and  $\gamma$ . The latter one is restricted to values near the electrovalence of the adsorbed specie. In comparison with the usual Monte Carlo approach, it is a reduced set of parameters, since in this approach, besides the parameters  $\gamma$  and  $\mu_{0C}$ , up to five lateral interaction between species is used in general [9].

Figure 2 shows the results of the fitting of eq. (41), with  $\eta$  given by (29) to (31), to experimental and simulated data for the electrosorption of  $Br$  in the surface of  $Ag(100)$  electrodes ([18], [19], [20]). We use a non-linear least squares fitting, applying the steepest descent procedure. Initial values for the parameters are estimated using eq. (38) and (42), and the  $Br$  electrovalence. The best fit results in  $\lambda = -47.7 \times 10^4$ ,  $\mu_{0C} = 610 meV$  and  $J = 44.6 meV$ . Although  $J$  and  $\mu_{0C}$  are strongly dependent on  $\gamma$ , the set of parameters gives a fit of the ratio  $i/(dV/dt)$  that is independent of  $\gamma$ . The surface coverage, nevertheless, depends on the value of the effective electrovalence, and it was used to fix  $\gamma = -0.73$ , which corresponds to the value given in [18] and gives a good agreement between the model and experimental data [19]. This value is also near the effective electrovalence estimated as  $\gamma = -0.71$  in [21], and no significative differences are found in the results computed with  $\gamma = -0.73$  or  $\gamma = -0.71$ . Experimental CVs present a shoulder followed by a sharp peak, this second corresponds to a phase transition from a disordered to an ordered phase [19]. The shoulder is attributed to configurational fluctuations on the  $Br$  adsorbed layer [18], and of course cannot be reproduced in the  $\phi^4$  model. Due the size of adsorbed bromine being bigger than the  $Ag(100)$  lattice spacing, in the ordered phase the bromine is distributed in an arrangement that covers only 50% of the  $Ag$  surface. Results for the surface coverage presented in figure 3 are normalized to reproduce this fact, and shows an reasonable agreement with the experimental data.

Figure 4 shows the results of the fitting of the model to experimental data for the Urea over  $Pt(100)$  surface [22]. Fitted parameters are  $\lambda = -58.4 \times 10^4$ ,  $\mu_{0C} = 97.8 meV$ ,  $\gamma = -1$  and  $J = 3.04 meV$ . Figure 5 shows the surface coverage for this process. In figure 4 the dotted line corresponds to the quadratic fitting of  $i^{-1}$ . We can see that there is an exceptional agreement between experimental data and the quadratic fitting in the sub critical potential region. Of course, this result is beyond the model presented here, since this quadratic solution do no take into account higher order terms in  $c$  on the solution of eq. (28).

On figure 5 the dashed horizontal lines correspond to the limits  $\langle \varphi \rangle = \eta = \pm \sqrt{J}/2$ , values of  $\eta$  inside this region and relatively far from these limits corresponds to the linear approximation of (19). As one can see from figures (4) and (5), the phase transition region is inside these limits. In particular, for the  $Br$  adsorption in  $Ag$ , all the voltammogram depicted on figure 2 is inside the region that corresponds to the linear approach.

Both results shows a good agreement between calculated and experimental/simulated data. The computational advantage of the field theoretical approach over the Monte Carlo simulation is the reduced number of parameters of the former.

## VI. CONCLUSION

In conclusion, we constructed a field theoretical model to describe electrochemical deposition. Based on the lattice-gas hamiltonian of the process, and taking a configurational mean of the occupation numbers, we obtained, in the continuous limit, a scalar field hamiltonian whose coefficients are related to the lattice-gas model effective quantities. Including higher order potential and treating the model in the mean field approximation, we obtain a single system of

equations ((20), (29)-(31) and (41)) that reproduces the current versus electrode potential behaviour in electrochemical deposition. The fitting of the model with experimental and numeric simulated data was obtained and shows a good agreement between model and experimental/simulated results. In comparison with the Monte Carlo approach, the model presented here has the advantage of presenting a reduced set of free parameters and simple analytical expressions for the observed quantities.

These results open the possibilities of new analytical description of other more complex deposition process, such as two species deposition, where one must use a two scalar field model, introducing new symmetries in the model (work in progress). Other even order potential terms could also be used to reproduce phase transitions between different ordered phases. They also suggests that the non-linear description of the process can presents other solutions, such as topological solutions like solitons and vortices. In fact, the  $\lambda\phi^4$  term can be viewed as a fourth order term in the expansion of a  $\cos(\phi)$  term in the lagrangian (19), leading to the sine-gordon model [23], which presents solitons.

Finally, the hamiltonian studied in this work shows us that the phase transition presented by electrochemical deposition is related to an explicitly symmetry breaking process, dictated by an external field (electrochemical potential), controlled by the electrode potential.

## VII. ACKNOWLEDGMENTS

The authors are grateful to CAPES-Brazil. We also thanks A. R. Pereira and M. C. Nemes for their suggestions to the present work.

- 
- [1] J. G. Dash and J. Ruvalds, *Phase Transition in Surface Physics*, (Plenum, New York, 1980).
  - [2] D. Nicholson and N. G. Parsonage, *Computer Simulation and the Statistical Mechanics of Adsorption*, (Academic Press, New York, 1982).
  - [3] D.P. Landau, *Phys. Rev. B* **27**, 5604 (1983).
  - [4] P.A. Rikvold, J.B. Collins, G.D. Hansen and J.D. Gunton, *Surf. Sci.* **203**, 500 (1988).
  - [5] J.B. Collins, P. Sacramento, P.A. Rikvold and J.D. Gunton, *Surf. Sci.* **221**, 277 (1989).
  - [6] P.A. Rikvold, M.R. Deakin, *Surf. Sci.* **294**, 180 (1991).
  - [7] M. Gamboa-Aldeco et. al., *Surf. Sci. Lett.* **221**, 297 (1993).
  - [8] P.A. Rikvold, M. Gamboa-Aldeco, J. Zhang, M. Han et. al., *Surf. Sci.* **335**, 389 (1995).
  - [9] P.A. Rikvold, J. Zhang, Y.E. Sung, A. Wieckowski, *Coll. Surf. A* **134**, 3 (1998).
  - [10] D.A. Huckaby and L. Blum, *J. Chem. Phys.* **92**, 2646 (1990).
  - [11] L. Blum and D.A. Huckaby, *J. Chem. Phys.* **94**, 6887 (1991).
  - [12] D.A. Huckaby and L. Blum, *J. Electroanal. Chem.* **315**, 255 (1991).
  - [13] D.A. Huckaby and L. Blum, *J. Electrochem. Soc. Conf. Proc.* **Ser.92-1**, 139 (1992).
  - [14] L. Blum and D.A. Huckaby, *J. Electrochem. Soc. Conf. Proc.* **Ser.93-5**, 139 (1993).
  - [15] L. Blum and D.A. Huckaby, *J. Electroanal. Chem.***375**, 69 (1994).
  - [16] L. Blum, D.A. Huckaby and M. Legaut, *Electrochem. Acta* **41**, 2207 (1996).
  - [17] G. Brown, P.A. Rikvold, S.J. Mitchell and M.A. Novotny, cond-mat/9805126
  - [18] S. Mitchell, G. Brown and P. A. Rikvold, *Surf. Sci.* **471**, 125 (2001).
  - [19] B.M. Ocko, J.X. Wang and T. Wandlowski, *Phys Rev Lett***79**,1511 (1997).
  - [20] G. Valette, A. Hamelin and R. Parsons, *Z Phys Chem* **113**, 71 (1978).
  - [21] I. Abou Hamad, Th. Wandlowski, G. Brown and P. A. Rikvold, *J. Electroanal. Chem.* **554-555**, 211 (2003).
  - [22] P.A. Rikvold, J. Zhang, Y.-E. Sung and A. Wieckowski, *Electrochem. Acta* **14**, 2184 (1996)..
  - [23] G.B. Whitham, *Linear and Nonlinear Waves*, Wiley, 1974.



## Figure Captions

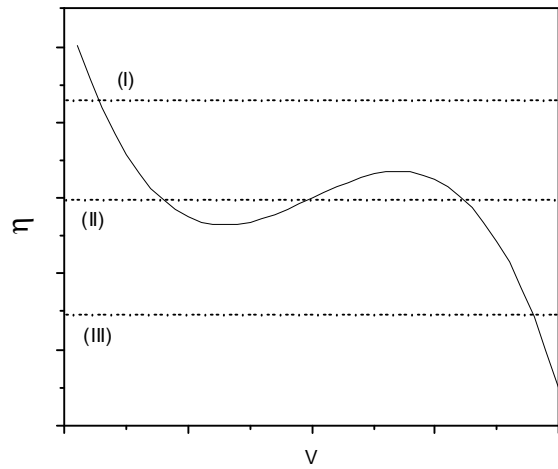
Figure 1: (a) Cubic equation corresponding for the configurational mean value of the occupation number  $\phi$ . The horizontal dashed lines correspond to the  $\eta = 0$  axis with I)  $c < 0$ , II)  $c = 0$  and III)  $c > 0$ . Note that for  $c > 0$  and  $c < 0$  one can have one or three real solutions. (b), (c) and (d) Potential energy as a function of  $\eta$  for different values of the symmetry breaking term. For  $c = 0$  the two minima are symmetric, as  $c$  goes from negative to positive values, the global minimum switches from one side to another, corresponding to the phase transition of the system.

Figure 2: Current density as a function of the electrode potential for the electrodeposition of  $Br$  on  $Ag(100)$  in the  $\phi^4$  model (solid line). Full and empty squares correspond to simulated results [18], empty squares are points not taken into account in the nonlinear fitting.

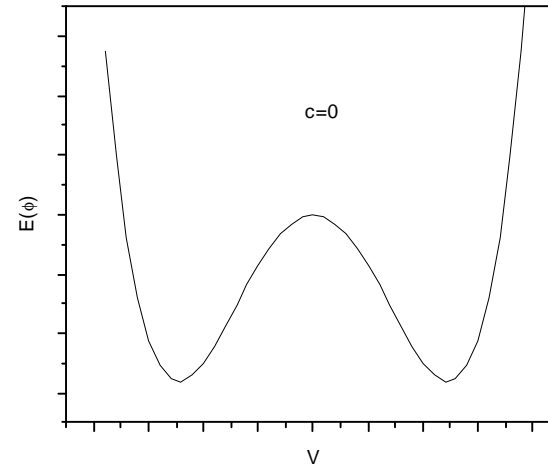
Figure 3:  $\phi^4$  model results (solid line) and experimental results (full squares) [19] for the surface coverage in the electrodeposition of  $Br$  on  $Ag(100)$ .

Figure 4: Current density as a function of the electrode potential for the electrodeposition of Urea on  $Pt(100)$  in the  $\phi^4$  model (solid line). Experimental results (full squares) are obtained from [22]. Dotted line corresponds to a quadratic polynomial fitting of  $i^{-1}$ .

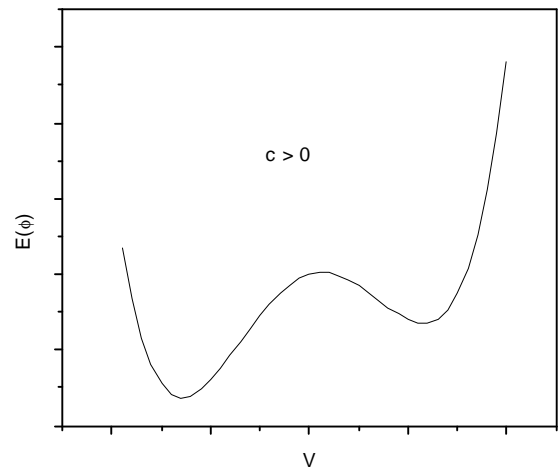
Figure 5: Surface coverage for the electrodeposition of Urea on  $Pt(100)$ . Dashed horizontal lines correspond to the approximate limits of the linear approach presented in this work.



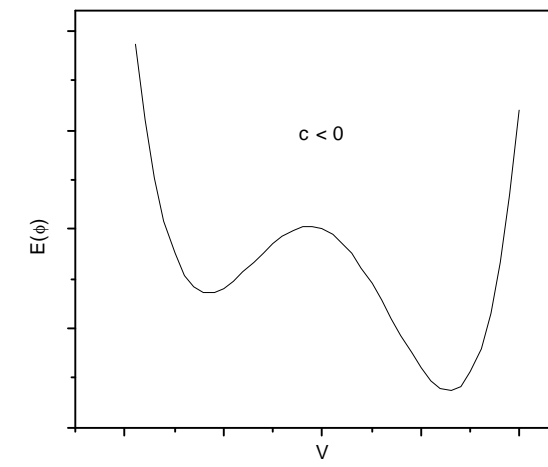
(a)



(b)



(c)



(d)

Figure 1

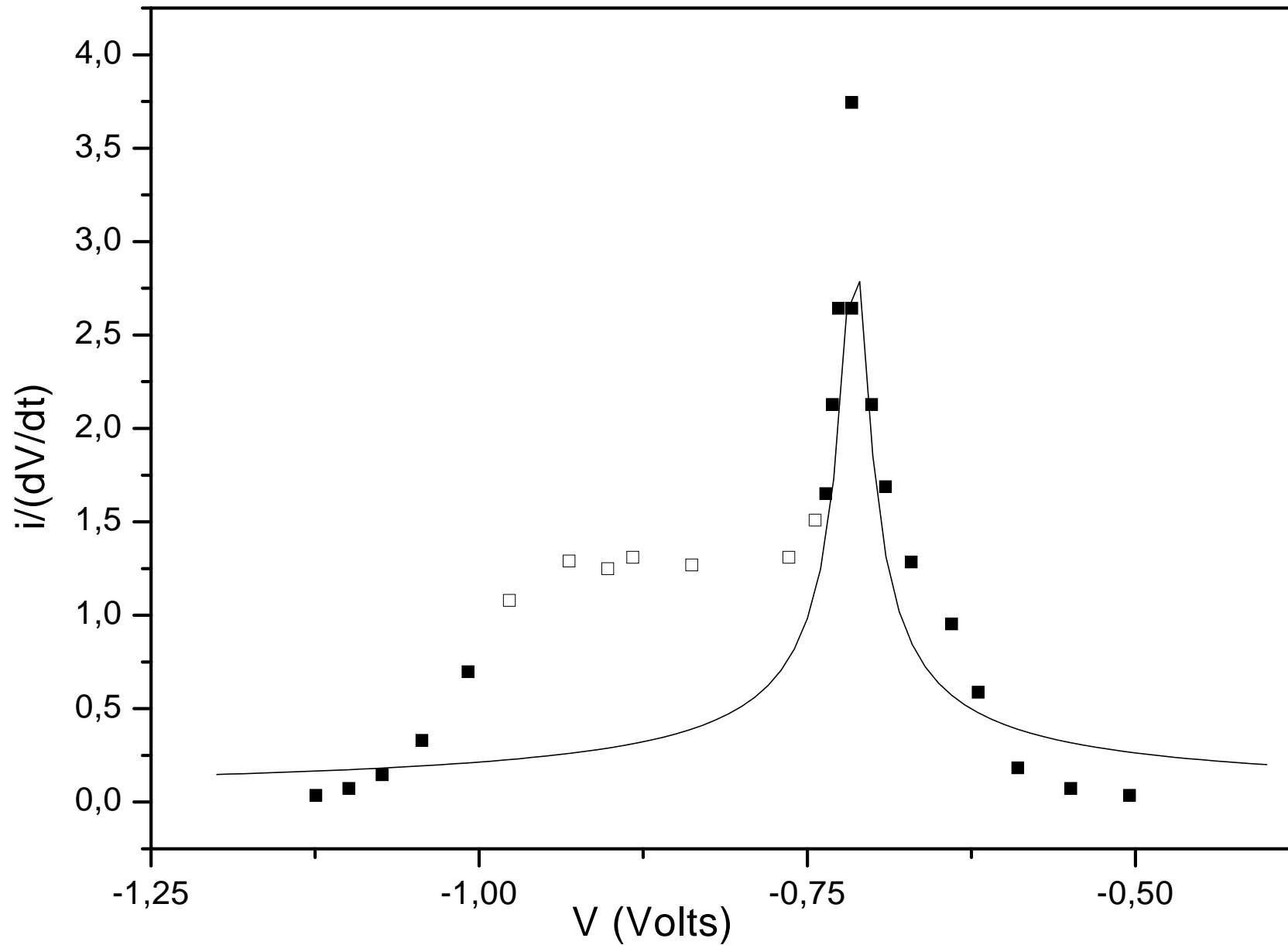


Figure 2

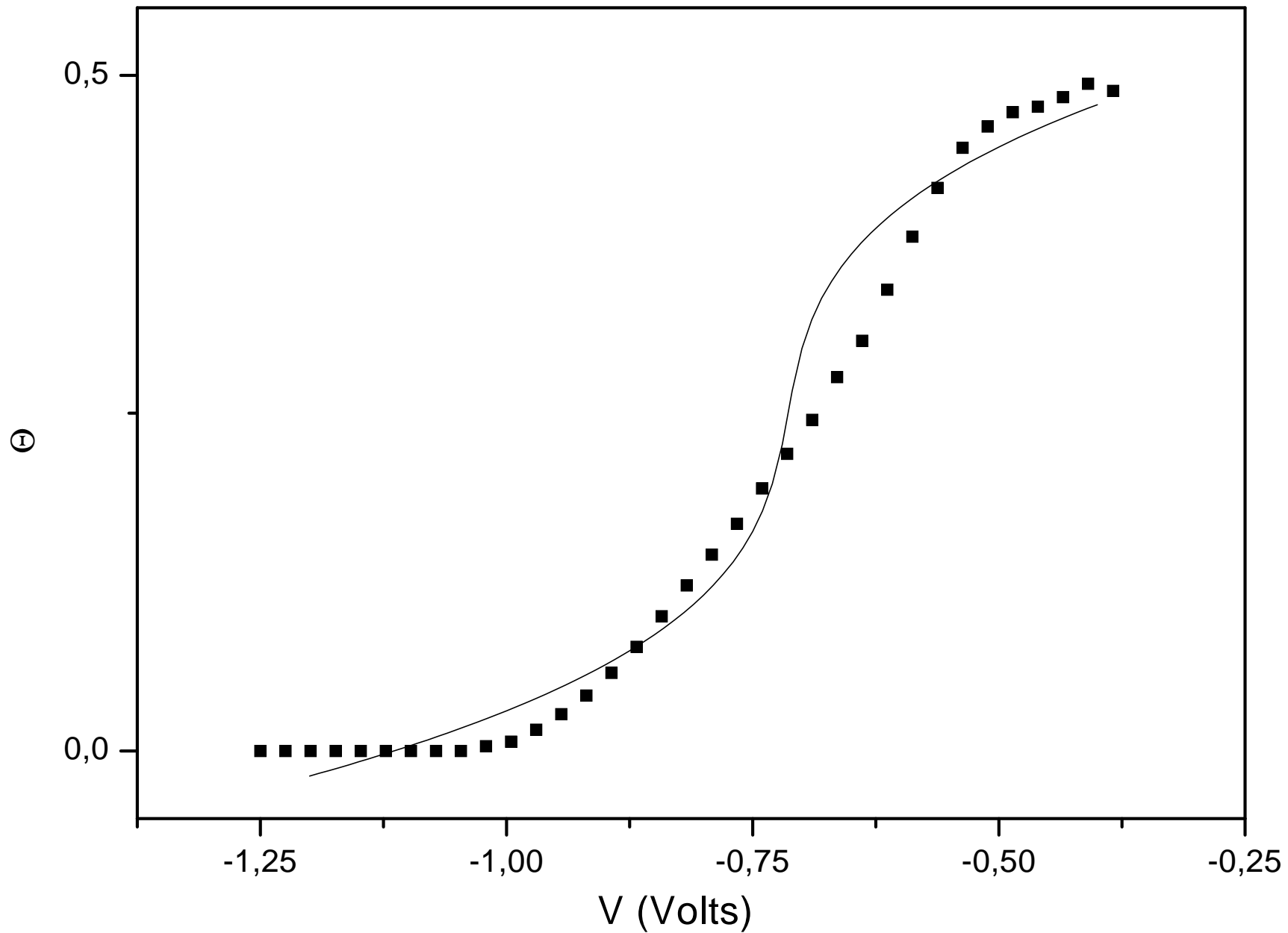


Figure 3

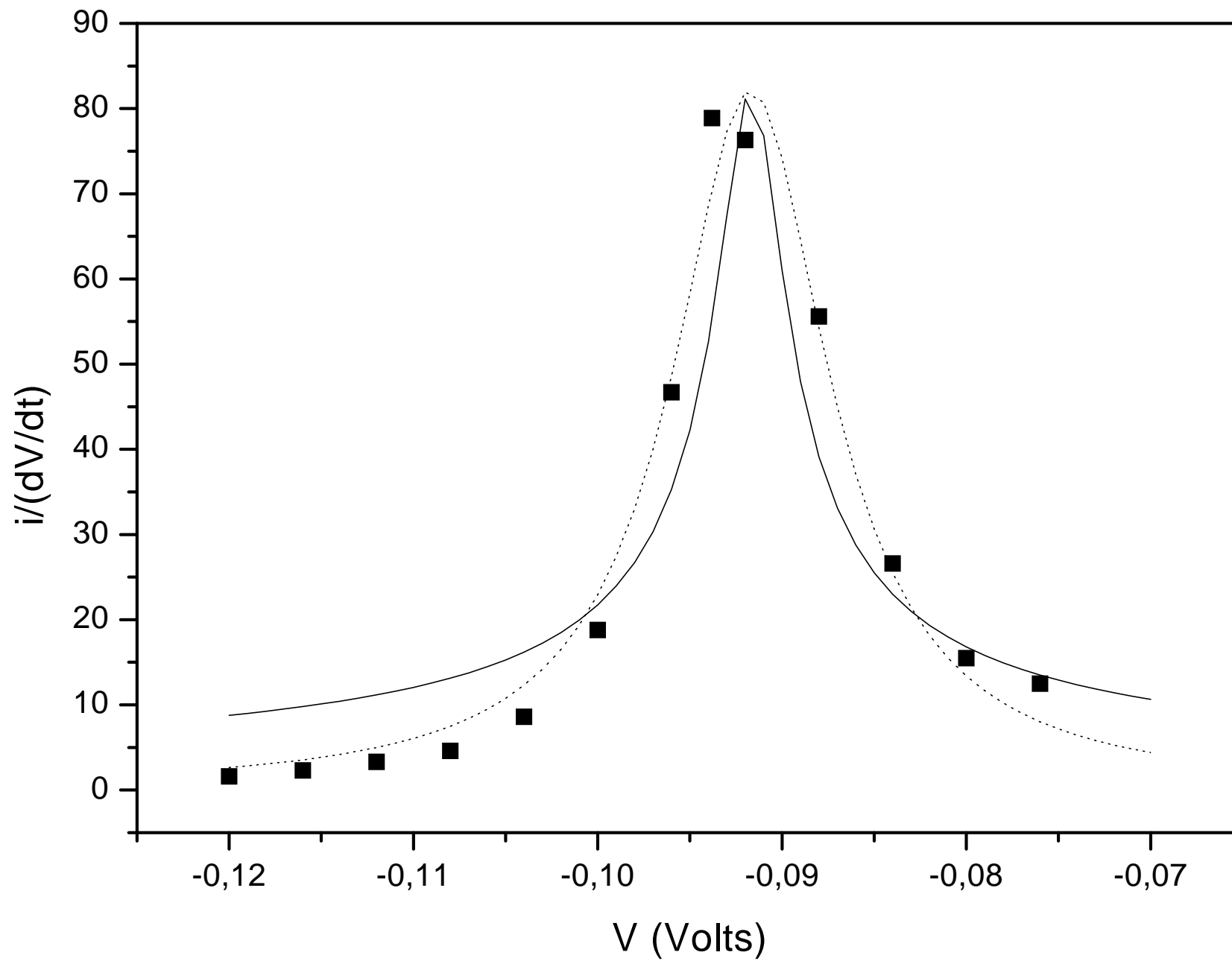
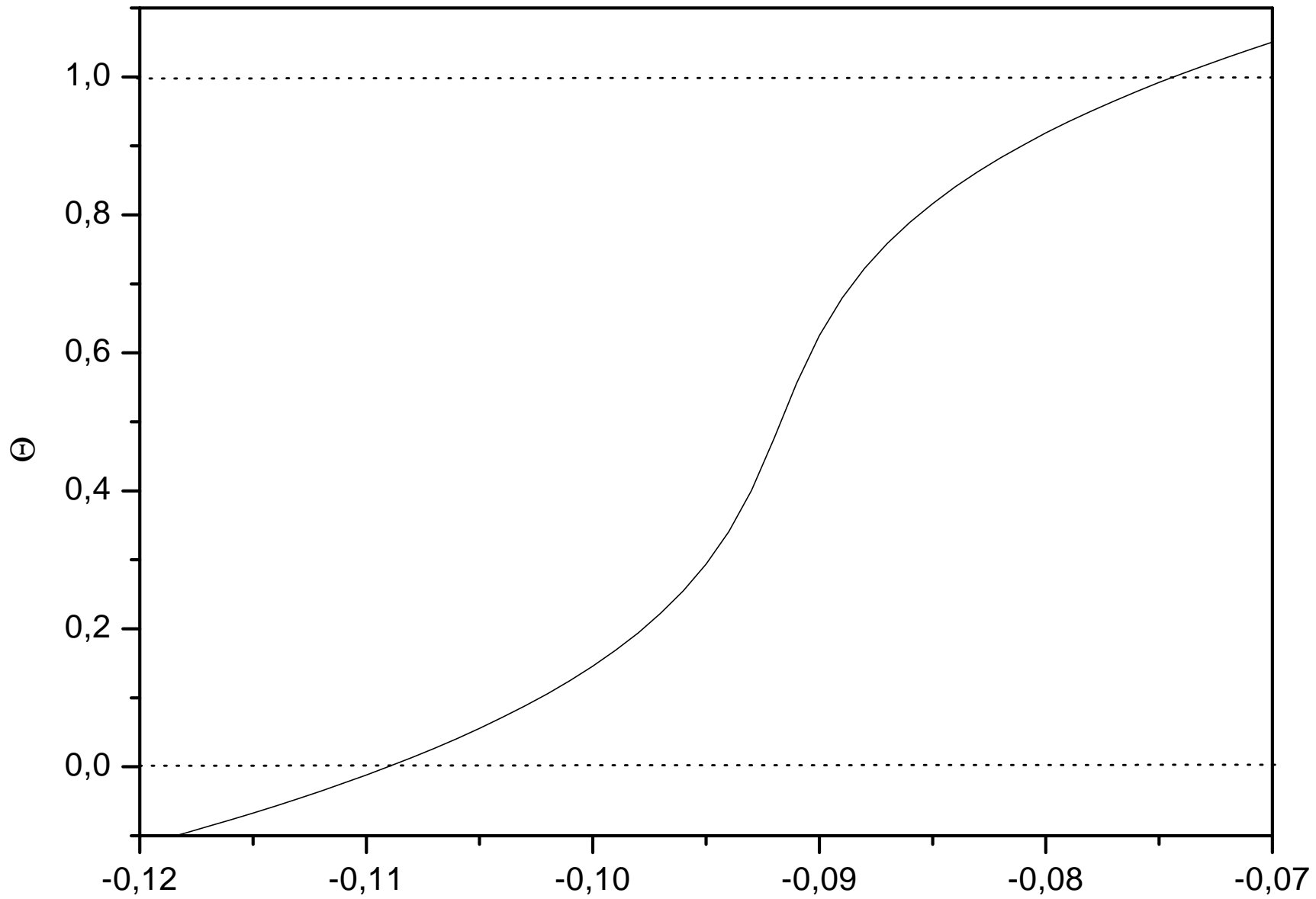


Figure 4



V (Volts)

Figure 5